

An Enhanced HSPICE Macromodel of a PCM Cell with Threshold Switching and Recovery Behavior

Linbin Chen and Fabrizio Lombardi

Electrical and Computer Engineering Department
Northeastern University
Boston, USA
lombardi@ece.neu.edu

Abstract— This paper proposes a new macromodel that takes into account the threshold switching and the resistance recovery processes in addition to the drift behavior of a Phase Change Memory (PCM). Simulation results are provided for both DC and drift behaviors; they show that the proposed macromodel is very accurate at a small error when compared with data from experimental devices. A sensitivity analysis of the macromodel is also performed to show its operation with respect to parameter variations. The model is suitable for circuit design based on PCM devices.

Index term – Phase-change memory, threshold switching, drift, recovery, modeling

I. INTRODUCTION

The Phase Change Memory (PCM) was first introduced by S. R. Ovshinsky in 1960 as a new type of non-volatile random-access memory (RAM). It exploits the unique behavior of the chalcogenide alloy; when heated by passing an electric current, this material changes between two states, crystalline and amorphous which are used to represent the binary bits value in memories. PCM is a promising candidate as a non-volatile memory among emerging technologies due to its good read/write times, high scalability, low power operation and good endurance.

Most of the recent papers on PCM modeling deal only with its DC characteristics. However, this analysis is limiting, because other features (such as, transient recovery and drift dynamics of the PCM resistance and threshold voltage [1]) are not fully analyzed. A comprehensive macromodel to include transient effects is essential for characterizing a PCM cell under different memory operations. This is particularly attractive when the drift behavior and its possible mitigation through recovery are considered.

This paper enhances [2] by proposing a new macromodel that takes into account the threshold switching and the resistance recovery processes in addition to the drift behavior of a PCM. The proposed macromodel is HSPICE compatible and takes into account DC and transient phenomena to ensure a very accurate assessment of the different parameters involved in the operation of a PCM cell. Simulation results are compared with experimental data to show that moderate errors are encountered and that the proposed macromodel is effective in assessing many operational features of a PCM inclusive of the resistance recovery process following the drift behavior. The paper is organized as follows. Section II briefly reviews the transient characteristics of the PCM, including threshold switching, recovery and drift of the resistance of the chalcogenide material. Section III introduces the enhanced

Jie Han

Electrical and Computer Engineering Department
University of Alberta
Edmonton, Canada
jhan8@ualberta.ca

HSPICE macromodel of the PCM. The transient simulation, error and sensitivity of the proposed macromodel to parameter variation is presented in section IV; Section VI concludes this manuscript.

II. REVIEW

A. Threshold Switching

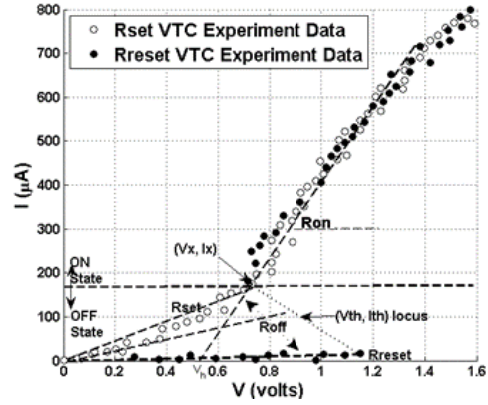


Fig. 1 Experimental I-V plot of a PCM [1]

A PCM cell consists of two steady-state regions i.e., ON and OFF. The transition from the OFF state to the ON state occurs when the voltage across the PCM cell is greater than V_{th} . V_{th} varies along the so-called V_{th} locus of the I-V plot of the PCM (Fig. 1). Moreover, the transition from the ON state to the OFF state occurs when the voltage across the PCM cell is less than V_x , where V_x is the intersection point of the R_{ON} curve and the R_{set} curve (Fig. 1). V_x is given by

$$V_x = V_h \cdot \frac{R_{set}}{R_{set} - R_{on}} \quad (1)$$

where V_h is the intersection of the R_{ON} curve and the horizontal voltage axis.

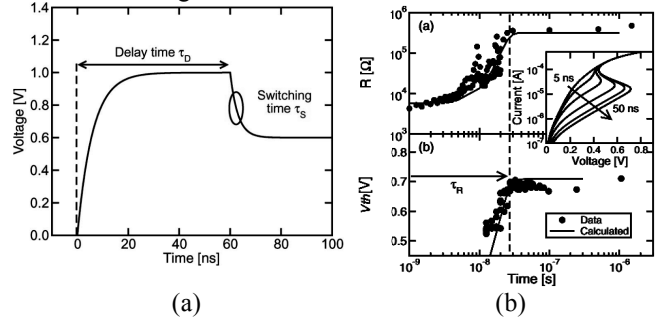


Fig. 2 (a) Time evolution of voltage across the PCM when a voltage pulse V_A is applied.[3] (b) Recovery dynamics of τ_R and V_{th} , and calculated transient curves [1]

The transition from the OFF state to the ON state exhibits an internal delay due to the underlying physical mechanism of

the threshold switching; a numerical/physical model of this delay has been developed in [3]. Fig. 2 (a) illustrates the definitions of the delay time τ_D and the switching transient delay τ_S . The switching time τ_S is the time required for the material to pass from the low-conductive OFF state to the highly-conductive ON state. Following the application of a voltage pulse V_A , the PCM requires a finite amount of time τ_D for accumulating a sufficient concentration of high-energy electrons for initiating threshold switching [4]. Both of the parameters are related to the physical properties of the chalcogenide alloy and are function of the applied voltage V_A [3].

B. Resistance Recovery

Usually, after a programming operation is completed, the PCM will change from the ON state to the OFF state. This transition occurs when the voltage across the PCM cell becomes lower than V_x in the ON state. V_x is the intersection point of the R_{sel} curve and the R_{ON} curve in the I-V plot of the PCM (Fig. 1). After the programming pulse is removed, the PCM does not suddenly quench to the low conductivity of the (intended) programmed R_{OFF} value, but it will experience a transition referred to as *recovery*. The time for recovering the intended R_{OFF} value is referred to as the recovery time and denoted by τ_R . During recovery, the amorphous conductivity is abnormally high (as result of an incomplete carrier relaxation to the equilibrium and excess temperatures [1]). Fig. 2 (b) illustrates the transition process of the PCM resistance and the threshold voltage at $\tau_R \approx 30\text{ns}$: a read operation prior to this time will clearly result in an erroneous value.

The time evolution of R_{OFF} following the removal of the programming pulse has been analyzed in the technical literature. A closed expression is given in [1] as

$$R_{OFF}(t_{OFF}) = R_{ON} e^{t_{OFF}/\tau} \quad (2)$$

where τ is the effective (constant) recombination time for excess carriers (typically 5ns [1]) and t_{OFF} is the time elapsed from the removal of the previous programming pulse. When t_{OFF} is equal to τ_R , the resistance $R_{OFF}(t_{OFF})$ reaches a saturation value, i.e. the intended value of R_{OFF} . Then, the PCM enters a process referred to as resistance drift due to its structural relaxation.

C. Drift Behavior

The drift behavior is given by the continuous value changing phenomenon in the OFF state after completing switching and recovery. The resistance and voltage characteristics of the OFF state (i.e., R_{OFF} and V_{th}) are time dependent. Several theoretical models have been proposed for the drift behavior of a PCM, such as for example the semi-classical band-model with valence alternation pairs (VAPs) formation [5], the trap-limited conduction model [6] and the stress release [7]. Regardless of the features of the models for the drift behavior, experimental data on R_{OFF} and V_{th} show that the drift operates under a constant annealing temperature and is described by the following equation,

$$R_{drift}(t_{OFF}) = R_0 \left(\frac{t_{OFF}}{t_0} \right)^v \quad (3)$$

where R_0 is the intended resistance due to programming and prior to the occurrence of the drift behavior. t_{OFF} is the time

when the PCM is not programmed. t_0 is a time constant. As indicated in [2], the drift coefficient v is related to the R_0 by,

$$v = \alpha \ln(R_0) - \beta \quad (4)$$

where α and β are curve fitting parameters. This equation indicate that the drift of R_{OFF} is more significant as the R_0 increases. v is considered as the most critical parameter when analyzing the drift behavior of a PCM cell.

The threshold voltage V_{th} also experiences a drift in value when the PCM is in the OFF state. Fig. 3 shows the measured V_{th} as function of R_{OFF} for different t_{OFF} values and at a fixed reset pulse [1]. Fig. 3 also shows the V_{th} - R_{OFF} plot for a variable reset voltage pulse and at $t_{OFF} = 5\text{s}$, i.e. V_{th} is linearly correlated to R_{OFF} under both scenarios.

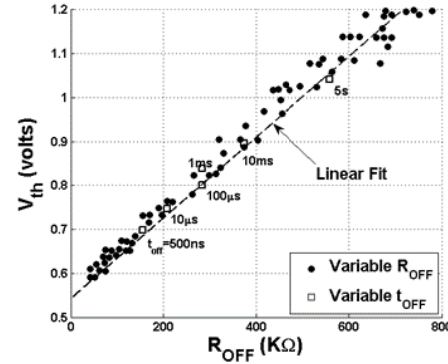


Fig. 3 V_{th} as function of R_{OFF} for variable t_{OFF} and fixed reset pulse [1]

III. ENHANCED MACROMODEL

The enhanced model of a PCM cell is shown in Fig. 4 in block form; it consists of different modules (the connections among modules are indicated by arrows); based on the model in [2], the added features or modification of the modules are shown as dotted boxes.

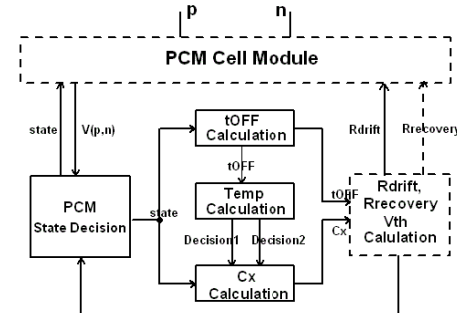


Fig. 4 Proposed macromodel of a PCM cell

In the proposed model, the PCM cell module is changed. [1] has been proved that following programming, the resistance dynamics of both the recovery and the drift can be combined together in a single resistance, i.e. by connecting R_{drift} and $R_{recovery}$ in parallel. So, the total transient evolution of R_{OFF} during the OFF state can be modeled as

$$R(t_{OFF}) = R_{drift}(t_{OFF}) || R_{recovery}(t_{OFF}) \quad (5)$$

Where

$$R_{recovery}(t_{OFF}) = R_{ON} e^{t_{OFF}/\tau} \quad (6)$$

The switching delay $\tau_D + \tau_S$ is modeled by connecting a capacitor C_{intern} in parallel with R_{OFF} . The value of the capacitor is selected according to experimental data ($\tau_D + \tau_S \approx 10n$ [3]). C_{intern} is set to 1pf by assuming that the switching delay will be completed within 5 time constants [3]. As shown in Fig. 5, R_{OFF} is represented in the proposed macromodel by two resistors connected in parallel, i.e. the equivalent resistor corresponds to the overall R_{OFF} of the PCM (as denoted by the dotted rectangle in Fig. 5).

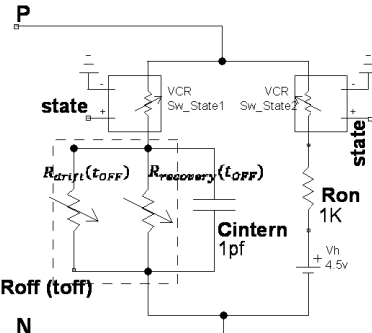


Fig. 5 PCM cell module

IV. MACROMODEL SIMULATION RESULTS

The HSPICE simulation results for the proposed DC and transient macromodel under the different operations of a PCM cell are presented next; the test circuit is shown in Fig. 6.

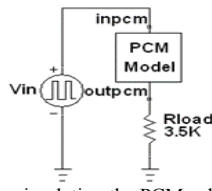


Fig. 6 Test circuit for simulating the PCM cell ($R_{\text{load}}=3.5\text{K}\Omega$ [8])

A. DC Analysis

Fig. 7 shows the comparison in I-V plots between the simulated results and the experimental data of [9] for DC analysis under the proposed macromodel of the PCM. An overall good agreement is found even though an error is encountered.

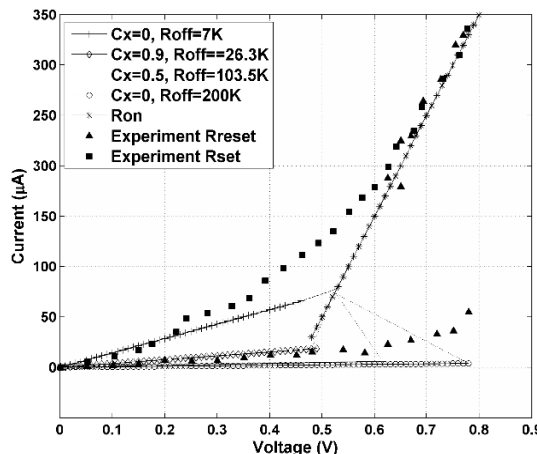


Fig. 7 Simulation and experimental [1] I-V plots of PCM cell

B. Transient simulation

Transient simulation is carried out to capture the threshold switching and recovery process. An input voltage source is imposed on the two terminal of the model p and n. The simulation results for the transient analysis of the proposed PCM macromodel are shown in Fig. 8; five timing diagrams are reported for the voltage across the PCM and the PCM resistance under different operations (write, read and recovery).

Fig. 8 (A) shows the input voltage $V_{PCM}=V(inPCM, outPCM)$ across the PCM in the test circuit of Fig. 6. Four types of pulses can be distinguished for the input voltage:

- *Crystalline Programming* pulses (fully crystalline programming: 1.2v, 200ns [10]. partial crystalline programming: 1.2v, 25ns)
- *Amorphous Programming* pulse (1.9v, 10ns [10])
- *Recovery* pulse (1v, 30ns)
- *Read* pulse (0.3v)

As required to switch the PCM to the ON state, the threshold voltage V_{th} is also shown, i.e. when the voltage across the PCM is above V_{th} , the PCM is in the ON state; when the voltage across the PCM is below V_x , the PCM is in the OFF state. V_{PCM} undergoes switching and recovery when a programming pulse is applied. Fig. 8 (B) shows the temperature under the pulses of V_{in} . For amorphous programming, the temperature rises above 873K[11]. For crystalline programming, the temperature is between 873K and 473K[11]. When the recovery pulse is applied, the temperature falls below 473K[11].

Fig. 8 (C) and (D) show the crystalline fraction and the resistance of the PCM as varying due to the different operations. The dotted line in (D) shows the ideal programmed resistance for each programming pulse. After each programming pulse, the ideal programmed resistance is not recovered at once, but it takes tens of nanoseconds to recover. Then following the recovery process, the resistance will drift according to the discussion presented in a previous section. In this figure, the fully crystalline programming pulse programs the resistance to $7\text{k}\Omega$ in about 200ns, while the amorphous programming pulse programs the resistance to R_{reset} ($200\text{k}\Omega$) in about 10ns.

The partial crystalline programming pulse for the intermediate resistance level programming is also shown in (D). The resistance can be programmed to any intermediate value by using a voltage pulse width (in this case 25ns) that is less than the fully crystalline programming pulse width. The recovery pulse makes the PCM to be in the ON state; however its voltage is not sufficiently high to start a phase change process (i.e. to reprogram the PCM). So after the application of a recovery pulse, the resistance recovers to the intended programmed value, i.e. the resistance drift that occurred since the last programming operation is corrected after the application of the recovery pulse. The read pulse has a very low voltage value (around 0.3v); so it does not turn on the PCM and the PCM remains in the OFF state during the read operation.

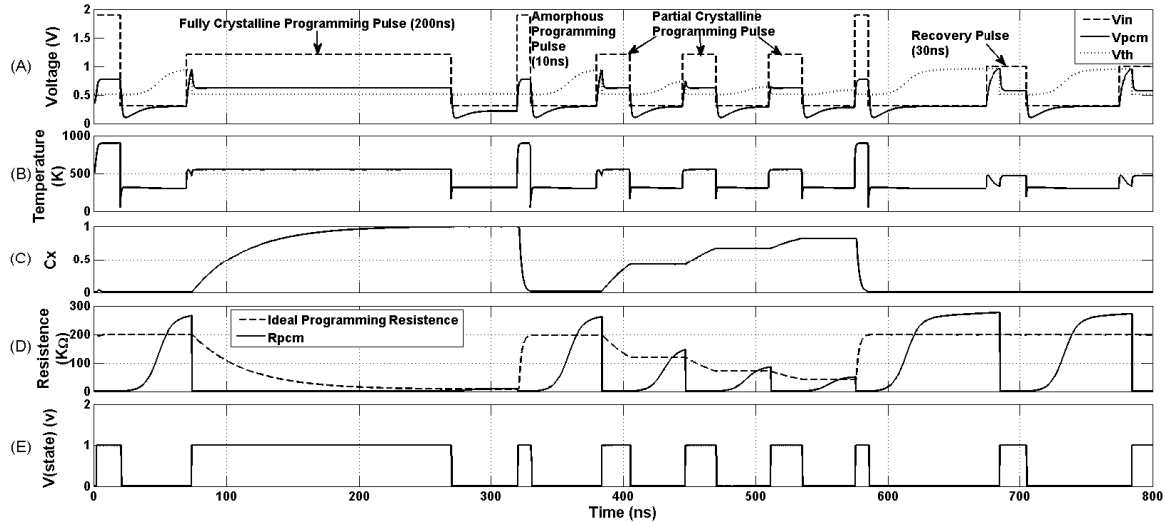


Fig. 8 Transient simulation of PCM Model

C. Error and Sensitivity

In this section, the error and sensitivity of the proposed model for transient operation is presented. Fig. 9 shows that the results of the macromodel of the recovery process are very close to the experimental data of [1], thus incurring only in a very small error of 4.26% on average (maximum errors (positive and negative values) are below 10%).

The recovery time τ_R is closely related to the time constant τ (i.e. the effective recombination time for excess carriers). The variation of τ ($\pm 10\%$) directly changes the recovery behavior, hence the recovery time τ_R (for 200K, $\pm 5.1\%$; for 7K, $\pm 1.2\%$).

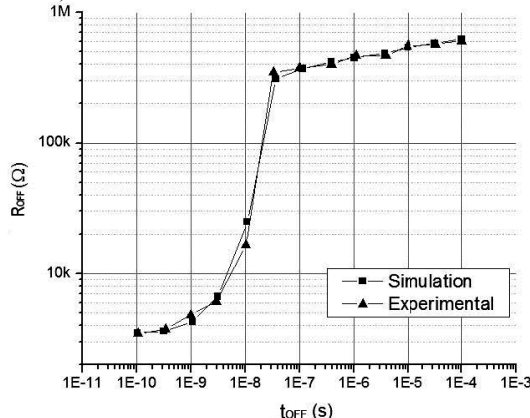


Fig. 9 Recovery process simulation results

V. CONCLUSION

This paper has proposed an enhanced HSPICE compatible macromodel for a PCM cell. This macromodel can capture both the DC and transient behaviors, thus being capable of assessing threshold switching and resistance drift recovery as transient and time dependent features of a PCM. It has been shown that using the macromodel the simulation results of different memory operations closely match the experimental data. Unlike the normal operations of a PCM, the recovery operation can be thought as a special case of the write operation in which a moderate programming pulse only turns on the device but it does not rewrite the resistance to the PCM.

- [1] D. Ielmini, L. L. Andrea, and M. Davide, "Recovery and Drift Dynamics of Resistance and Threshold Voltages in Phase-Change Memories," *Electron Devices, IEEE Transactions on*, vol. 54, pp. 308-315, 2007.
- [2] P. Junsangsri, J. Han, and F. Lombardi, "On the drift behaviors of a phase change memory (PCM) cell," in *Nanotechnology (IEEE-NANO), 2013 13th IEEE Conference on*, 2013, pp. 1145-1150.
- [3] S. Lavizzari, D. Ielmini, and A. L. Lacaita, "Transient Simulation of Delay and Switching Effects in Phase-Change Memories," *Electron Devices, IEEE Transactions on*, vol. 57, pp. 3257-3264, 2010.
- [4] D. Ielmini and Y. Zhang, "Analytical model for subthreshold conduction and threshold switching in chalcogenide-based memory devices," *Journal of Applied Physics*, vol. 102, pp. 054517-054517-13, 2007.
- [5] A. Pirovano, A. L. Lacaita, F. Pellizzer, S. A. Kostylev, A. Benvenuti, and R. Bez, "Low-field amorphous state resistance and threshold voltage drift in chalcogenide materials," *Electron Devices, IEEE Transactions on*, vol. 51, pp. 714-719, 2004.
- [6] S. Lavizzari, D. Ielmini, D. Sharma, and A. L. Lacaita, "Reliability Impact of Chalcogenide-Structure Relaxation in Phase-Change Memory (PCM) Cells - Part II: Physics-Based Modeling," *Electron Devices, IEEE Transactions on*, vol. 56, pp. 1078-1085, 2009.
- [7] I. V. Karlov, M. Mitra, D. Kau, G. Spadini, Y. A. Kryukov, and V. G. Karlov, "Fundamental drift of parameters in chalcogenide phase change memory," *Journal of Applied Physics*, vol. 102, p. 124503, 2007.
- [8] D. Ielmini, A. L. Lacaita, D. Mantegazza, F. Pellizzer, and A. Pirovano, "Assessment of threshold switching dynamics in phase-change chalcogenide memories," in *Electron Devices Meeting, 2005. IEDM Technical Digest. IEEE International*, 2005, pp. 877-880.
- [9] D. Ielmini, A. L. Lacaita, A. Pirovano, F. Pellizzer, and R. Bez, "Analysis of phase distribution in phase-change nonvolatile memories," *Electron Device Letters, IEEE*, vol. 25, pp. 507-509, 2004.
- [10] Y.-B. Liao, J.-T. Lin, and M.-H. Chiang, "Temperature-based phase change memory model for pulsing scheme assessment," in *Integrated Circuit Design and Technology and Tutorial, 2008. ICICDT 2008. IEEE International Conference on*, 2008, pp. 199-202.
- [11] D.-L. Cai, Z.-T. Song, X. Li, H.-P. Chen, and X.-G. Chen, "A Compact Spice Model with Verilog-A for Phase Change Memory," *Chinese Physics Letters*, vol. 28, p. 018501, 2011.